



# CALCULATION OF STEAM DROP MIXTURE FLOWS WITH BOILING EXPLOSION MECHANISM USING A MULTIDIMENSIONAL NODAL METHOD OF CHARACTERISTICS

V.S. Surov

*South Ural State University (NRU), Chelyabinsk, Russian Federation*

A hyperbolic model of a vapor-drop mixture is presented that takes into account the evaporation of drops by an explosive mechanism. The model is developed on the basis of the generalized equilibrium model of a mixture proposed by the author earlier. To hyperbolize the equations, forces of interfractional interaction are introduced. The liquid fraction was assumed to be incompressible. In the model used, it was assumed that the phase transition in the process of intense evaporation of droplets occurs under conditions of an overheated state when the liquid temperature exceeds the saturation temperature. A characteristic analysis of the model equations was carried out, and their hyperbolicity was shown. An analytical formula was obtained for determining the speed of sound in a vapor-drop mixture. It is noted that the speed of sound in the mixture in the presence of phase transformations turns out to be somewhat smaller than that given by Wood's formula. A multidimensional nodal characteristic method is described, intended for integrating hyperbolic systems, which is based on splitting the original system of equations into a number of one-dimensional subsystems. Differential relations are derived that are valid in the characteristic directions for each of the subsystems. When calculating one-dimensional problems, an iterative algorithm of the inverse method of characteristics was applied. The computational method has been tested on a number of problems with self-similar solutions. The flow of a vapor-droplet flow near the disk was studied using the chosen method of integration of the multidimensional system of equations. It is shown that in some cases, it is necessary to take into account the explosive boiling of liquid droplets since it can significantly change the pattern of flow around the disk.

**Key words:** vapor droplet mixture, hyperbolic model, multidimensional node method of characteristics

## 1. Introduction

A model of a vapor-droplet mixture is presented, in which the evaporation of drops by the mechanism of explosive boiling is taken into account. The single-velocity generalized equilibrium (GR) hyperbolic two-temperature model from [1] was taken as the basis. Previously, the GR model was used by the author in modeling wave processes in foamed liquids and bubbly media [2], in studying the flows of viscous heat-conducting mixtures (in this case, instead of the original Fourier and Stokes laws, their relaxation analogs were used [3]), and for localizing contact surfaces in multifluid hydrodynamics. The results discussed in this paper indicate that the GR model is also suitable for studying multidimensional flows in the presence of phase transformations by the mechanism of explosive (volumetric) liquid boiling; it is shown that the type of the system of equations does not change — it remains hyperbolic. The conservation of hyperbolicity makes it possible, in particular, to find an analytical expression for the velocity of sound waves in a mixture in the presence of phase transformations. Solutions of one-dimensional problems within the framework of this model were carried out in [4]. It should be noted that the explosive boiling model was previously used to simulate an overheated liquid under conditions of a sharp change in external pressure, for example, during pipeline depressurization [5], but not to study flow of the vapor-drop mixture. However, the op model can also be used to calculate flow parameters with another mechanism of phase transformation — surface evaporation from media interfaces [6–8]. For rather "small" droplets, which are the main object of study, the one-velocity approximation is justified. This is confirmed in [9], where a direct comparison was made with the results of solving a problem close to the one considered in this article, described by a one-velocity model and a model that takes into account velocity nonequilibrium. Integration of the model equations is carried out by the method of characteristics (MC), the essence of which is the transition from differential equations in partial derivatives to ordinary differential equations, which are written along the characteristic directions. Various schemes of multidimensional MC are given in [10].

In the work presented to the reader's attention, a variant of the multidimensional MC is used, based on the splitting of the original system of equations in space variables into a number of one-dimensional subsystems with their subsequent integration using the one-dimensional nodal MC [11]. This method of splitting in

directions is similar to the approach from [12]. Unlike the well-known method of fractional steps [13], fractional time steps are not used in the algorithm. It is important that, despite the number of arithmetic operations performed in the multidimensional nodal mx described below than in a number of finite-difference or finite-volume methods, the total computational time often turns out to be significantly less due to a larger time step. In addition, the software implementation of multidimensional nodal MC is much simpler than many finite-volume methods due to the absence of a laborious procedure for constructing grids in the computational domain with the subsequent solution of Riemann problems on the faces of adjacent cells, for example, as in the Godunov method, which is especially important for problems with complex geometry of the computational domain.

## 2. Steam-droplet mixture model

The equations describing the axisymmetric flow of a single-velocity vapor-drop mixture, in which, for simplicity, the liquid is assumed to be incompressible (in [14], this approximation was removed) in the presence of phase transformations and expressing the laws of conservation of mass, momentum, and energy for each of the fractions that make up the mixture in divergent form, have the form:

$$\begin{aligned}
 & \frac{\partial \alpha_{st} \rho_{st}^0}{\partial t} + \frac{\partial \alpha_{st} \rho_{st}^0 u}{\partial x} + \frac{\partial \alpha_{st} \rho_{st}^0 v}{\partial r} + \frac{\alpha_{st} \rho_{st}^0 v}{r} = J, \\
 & \frac{\partial \alpha_{st} \rho_{st}^0 u}{\partial t} + \frac{\partial \alpha_{st} (p + \rho_{st}^0 u^2)}{\partial x} + \frac{\partial \alpha_{st} \rho_{st}^0 uv}{\partial r} + \frac{\alpha_{st} \rho_{st}^0 uv}{r} = f_x + Ju, \\
 & \frac{\partial \alpha_{st} \rho_{st}^0 v}{\partial t} + \frac{\partial \alpha_{st} \rho_{st}^0 vu}{\partial x} + \frac{\partial \alpha_{st} (p + \rho_{st}^0 v^2)}{\partial r} + \frac{\alpha_{st} \rho_{st}^0 v^2}{r} = f_r + Jv, \\
 & \frac{\partial \alpha_{st} \rho_{st}^0 e_{st}}{\partial t} + \frac{\partial \alpha_{st} u (\rho_{st}^0 e_{st} + p)}{\partial x} + \frac{\partial \alpha_{st} v (\rho_{st}^0 e_{st} + p)}{\partial r} + \frac{\alpha_{st} v (\rho_{st}^0 e_{st} + p)}{r} = f_x u + f_r v + J e_s, \\
 & \frac{\partial \alpha_s \rho_s^0}{\partial t} + \frac{\partial \alpha_s \rho_s^0 u}{\partial x} + \frac{\partial \alpha_s \rho_s^0 v}{\partial r} + \frac{\alpha_s \rho_s^0 v}{r} = -J, \\
 & \frac{\partial \alpha_s \rho_s^0 u}{\partial t} + \frac{\partial \alpha_s (p + \rho_s^0 u^2)}{\partial x} + \frac{\partial \alpha_s \rho_s^0 vu}{\partial r} + \frac{\alpha_s \rho_s^0 vu}{r} = -f_x - Ju, \\
 & \frac{\partial \alpha_s \rho_s^0 v}{\partial t} + \frac{\partial \alpha_s \rho_s^0 u^2}{\partial x} + \frac{\partial \alpha_s (p + \rho_s^0 v^2)}{\partial r} + \frac{\alpha_s \rho_s^0 v^2}{r} = -f_r - Jv, \\
 & \frac{\partial \alpha_s \rho_s^0 e_s}{\partial t} + \frac{\partial \alpha_s u (\rho_s^0 e_s + p)}{\partial x} + \frac{\partial \alpha_s v (\rho_s^0 e_s + p)}{\partial r} + \frac{\alpha_s v (\rho_s^0 e_s + p)}{r} = -f_x u - f_r v - J e_s,
 \end{aligned} \tag{1}$$

where  $p$  is pressure;  $u$  and  $v$  are the components of the velocity vector in the direction of the symmetry axes  $Ox$  and  $Or$ ;  $J$  – the intensity of vaporization per unit volume of the mixture;  $\mathbf{f}$  is the density vector of the force of interfractional interaction with the components  $(f_x, f_r)$ , which ensures the absence of relative slippage of fractions, which is unknown in advance and is determined in the process of integrating system (1) [1];  $\alpha_i$  is the volume fraction of the  $i$ -th fraction in the mixture ( $i = s, st$ ),  $\alpha_{st} + \alpha_s = 1$ ;  $\rho_i^0$  — the physical density of the  $i$ -th component;  $e_i = \varepsilon_i + \frac{u^2 + v^2}{2}$  — specific total energies;  $\varepsilon_{st} = \varepsilon_{st}(p, \rho_{st}^0)$  and  $\varepsilon_s = c_{v,s} \theta_s + \varepsilon_{s0}$  are the specific internal energies of steam and incompressible fractions;  $c_{v,s}$  — the heat capacity of the liquid;  $\theta_s$  — the temperature of the dispersed fraction. The indices  $s$  and  $st$  denote the incompressible fraction and vapor, respectively. It is important that if the force of interfractional interaction is not included in the equations of the model, then system (1) loses the property of hyperbolicity [1]. In this work, processes were studied at rather short time intervals, measured in milliseconds, so interfractional heat transfer was not taken into account. The intensity of the water–steam phase transition was calculated from the relation [15]:

$$J = 2\pi a n \rho_{st}^0 D_s \text{Ja Nu}, \tag{2}$$

where the dimensionless Jacob and Nusselt numbers were determined from the expressions

$$\text{Ja} = \frac{c_s \rho_s^0}{h \rho_{st}^0} [\theta_s - \theta_N(p)], \quad \text{Nu} = 2 + \left( \frac{6 \text{Ja}}{\pi} \right)^{1/3} + \frac{12 \text{Ja}}{\pi}.$$

In (2), the following designations are adopted:  $D_s = \frac{\lambda_s}{c_s \rho_s^0}$  — the coefficient of thermal conductivity;  $\lambda_s$  and  $c_s$  — the thermal conductivity and heat capacity of the liquid;  $h$  — the specific heat of vaporization;  $a$  — the radius of the drop (for simplification, we assume that all drops have the same size);  $n$  — the number of drops per unit volume of the mixture. The last two parameters are related to the volume fraction of the liquid fraction in the mixture by the ratio  $\alpha_s = \frac{4}{3} \pi n a^3$ . Saturation temperature  $\theta_N(p)$  was determined from the expression

$$\theta_N(p) = \theta_{..} - \frac{\theta_{..}}{\ln(p/p_{..})},$$

where for water:  $p_{..} = 20,2 \times 10^9 \text{ Pa}$ ,  $\theta_{..} = 4200 \text{ K}$ ,  $\theta_{..} = 31 \text{ K}$  [16]. The calculations assumed that the phase transition in the process of explosive boiling of droplets occurs in an overheated state when the temperature of the liquid exceeds the saturation temperature, that is, at  $\theta_s - \theta_N(p) > \Delta\theta_s$ , where  $\Delta\theta_s$  — overheating of the liquid.

Summing up the corresponding conservation laws for the fractions composing the mixture, we obtain the conservation laws of mass, momentum and energy for the mixture as a whole:

$$\begin{aligned} \frac{\partial \rho}{\partial t} + \frac{\partial \rho u}{\partial x} + \frac{\partial \rho v}{\partial r} + \frac{\rho v}{r} = 0, \quad \frac{\partial \rho u}{\partial t} + \frac{\partial (p + \rho u^2)}{\partial x} + \frac{\partial \rho u v}{\partial r} + \frac{\rho u v}{r} = 0, \\ \frac{\partial \rho v}{\partial t} + \frac{\partial \rho u v}{\partial x} + \frac{\partial (p + \rho v^2)}{\partial r} + \frac{\rho v^2}{r} = 0, \\ \frac{\partial \rho e}{\partial t} + \frac{\partial u(\rho e + p)}{\partial x} + \frac{\partial v(\rho e + p)}{\partial r} + \frac{v(\rho e + p)}{r} = 0. \end{aligned} \quad (3)$$

Here,  $\rho = \alpha_{st} \rho_{st}^0 + \alpha_s \rho_s^0$  is the density of the mixture;  $\varepsilon = \frac{1}{\rho} (\alpha_{st} \rho_{st}^0 \varepsilon_{st} + \alpha_s \rho_s^0 \varepsilon_s)$  and  $e = \varepsilon + \frac{u^2 + v^2}{2}$  — the specific internal and total energy of the mixture per unit volume. Equations (3) in quasilinear form have the form

$$\frac{1}{\rho} \frac{D\rho}{Dt} + \frac{\partial u}{\partial x} + \frac{\partial v}{\partial r} + \frac{v}{r} = 0, \quad \frac{Du}{Dt} + \frac{1}{\rho} \frac{\partial p}{\partial x} = 0, \quad \frac{Dv}{Dt} + \frac{1}{\rho} \frac{\partial p}{\partial r} = 0, \quad \frac{D\varepsilon}{Dt} - \frac{p}{\rho^2} \frac{D\rho}{Dt} = 0.$$

Here,  $\frac{D}{Dt} = \frac{\partial}{\partial t} + u \frac{\partial}{\partial x} + v \frac{\partial}{\partial r}$ . The corresponding conservation laws for vapor and liquid from (1) will take the form

$$\begin{aligned} \frac{D\rho_{st}}{Dt} = \frac{\rho_{st}}{\rho} \frac{D\rho}{Dt} + J, \quad \rho_{st} \frac{Du}{Dt} + \frac{\partial \alpha_{st} p}{\partial x} = f_x, \\ \rho_{st} \frac{Dv}{Dt} + \frac{\partial \alpha_{st} p}{\partial r} = f_r, \quad \rho_{st} \frac{D\varepsilon_{st}}{Dt} - \frac{\alpha_{st} p}{\rho} \frac{D\rho}{Dt} = J(\varepsilon_s - \varepsilon_{st}), \\ \frac{D\alpha_s}{Dt} = \frac{\alpha_s}{\rho} \frac{D\rho}{Dt} - \frac{J}{\rho_s^0}, \quad \rho_s \frac{Du}{Dt} + \frac{\partial \alpha_s p}{\partial x} = -f_x, \end{aligned}$$

$$\rho_s \frac{Dv}{Dt} + \frac{\partial \alpha_s p}{\partial r} = -f_r, \quad \frac{D\varepsilon_s}{Dt} = \frac{p}{\rho \rho_s^0} \frac{D\rho}{Dt} + \frac{J}{2\rho_s} (u^2 + v^2).$$

Here,  $\rho_k = \alpha_k \rho_k^0$  is the reduced density of the  $k$ -th fraction ( $k = s$  and  $st$ ). Considering the equality

$$\frac{D\varepsilon_{st}}{Dt} = \frac{\partial \varepsilon_{st}}{\partial p} \frac{Dp}{Dt} + \frac{\partial \varepsilon_{st}}{\partial \rho_{st}^0} \frac{D\rho_{st}^0}{Dt}, \quad \frac{D\alpha_{st}}{Dt} = \frac{J}{\rho_s^0} - \frac{\alpha_s}{\rho} \frac{D\rho}{Dt}, \quad \frac{D\rho_{st}^0}{Dt} = \frac{1}{\alpha_{st}} \left[ \frac{D\rho}{Dt} - (\rho_s^0 - \rho_{st}^0) \frac{D\alpha_s}{Dt} \right],$$

the law of conservation of energy for the mixture as a whole can be rewritten as

$$\frac{Dp}{Dt} - c^2 \frac{D\rho}{Dt} = \Pi,$$

Here

$$c^2 = \left( p - \frac{\rho_{st}^{02}}{\alpha_{st}} \frac{\partial \varepsilon_{st}}{\partial \rho_{st}^0} \right) \left( \rho \rho_{st}^0 \frac{\partial \varepsilon_{st}}{\partial p} \right)^{-1}, \quad (4)$$

$$\Pi = J \left[ \varepsilon_s - \varepsilon_{st} + \frac{\rho_{st}^0}{\rho_s^0} \frac{\partial \varepsilon_{st}}{\partial \rho_{st}^0} (\rho_s^0 - \rho_{st}^0) - \frac{u^2 + v^2}{2} \right] \left( \alpha_{st} \rho_{st}^0 \frac{\partial \varepsilon_{st}}{\partial p} \right)^{-1}.$$

Here,  $c$  is the speed of sound in the mixture. Thus, the equations of axisymmetric motion of a vapor-droplet mixture in the presence of phase transformations in a quasilinear form take the form

$$\begin{aligned} \frac{\partial \rho}{\partial t} + u \frac{\partial \rho}{\partial x} + v \frac{\partial \rho}{\partial r} + \rho \left( \frac{\partial u}{\partial x} + \frac{\partial v}{\partial r} + \frac{v}{r} \right) &= 0, \\ \frac{\partial u}{\partial t} + u \frac{\partial u}{\partial x} + v \frac{\partial u}{\partial r} + \frac{1}{\rho} \frac{\partial p}{\partial x} &= 0, \quad \frac{\partial v}{\partial t} + u \frac{\partial v}{\partial x} + v \frac{\partial v}{\partial r} + \frac{1}{\rho} \frac{\partial p}{\partial r} &= 0, \\ \frac{\partial p}{\partial t} + u \frac{\partial p}{\partial x} + v \frac{\partial p}{\partial r} + \rho c^2 \left( \frac{\partial u}{\partial x} + \frac{\partial v}{\partial r} + \frac{v}{r} \right) &= \Pi, \quad (5) \\ \frac{\partial \alpha_s}{\partial t} + u \frac{\partial \alpha_s}{\partial x} + v \frac{\partial \alpha_s}{\partial r} + \alpha_s \left( \frac{\partial u}{\partial x} + \frac{\partial v}{\partial r} + \frac{v}{r} \right) &= -\frac{J}{\rho_s^0}, \\ \frac{\partial \theta_s}{\partial t} + u \frac{\partial \theta_s}{\partial x} + v \frac{\partial \theta_s}{\partial r} + \frac{p}{c_{v,s} \rho_s^0} \left( \frac{\partial u}{\partial x} + \frac{\partial v}{\partial r} + \frac{v}{r} \right) &= \frac{u^2 + v^2}{\alpha_s c_{v,s} \rho_s^0} J. \end{aligned}$$

The roots of the characteristic equation of system (5) are real numbers. In addition, the eigenvectors corresponding to the eigenvalues of the system are linearly independent; therefore, system (5) belongs to the hyperbolic type [17]. In addition, in (5), there are no densities of forces of interfractional interaction. If necessary, they can be found from the original system of equations (1).

The following were used as the caloric and thermal equations of state of water vapor:

$$\varepsilon_{st} = \frac{(p + \gamma_{st} p_{st})(1 - \rho_{st}^0 b_{st})}{(\gamma_{st} - 1) \rho_{st}^0} + q_{st}, \quad \theta_{st} = \frac{(p + p_{st})(1 - \rho_{st}^0 b_{st})}{(\gamma_{st} - 1) \rho_{st}^0 c_{v,st}}, \quad (6)$$

where  $\gamma_{st} = 1,47$ ;  $p_{st} = 0$ ;  $q_{st} = 2,077616 \times 10^6$  J/kg;  $c_{v,st} = 0,955 \times 10^3$  J/(kg K); and  $b_{st} = 0$  [18]. The relations from [19] were also used:

$$\varepsilon_{st} = c_{v,st} \theta_{st} + \varepsilon_{st}^{ch}, \quad p = R_{st} \rho_{st}^0 \theta_{st}, \quad (7)$$

valid at pressures less than 10 atm. Here,  $c_{v,st}^* = 1,43 \times 10^3$  J/(kg K);  $R_{st} = 461,7$  J/(kg K);  $\varepsilon_{st}^{ch} = 1,93 \times 10^6$  J/kg. Expressions for the square of the speed of sound from (4), in the case of using (6) and (7), take the form, respectively:

$$c^2 = \frac{p(\gamma_{st} + \alpha_s/\alpha_{st})}{\rho}, \quad c_*^2 = \frac{p(R_{st}/c_{v,st}^* + 1/\alpha_{st})}{\rho}.$$

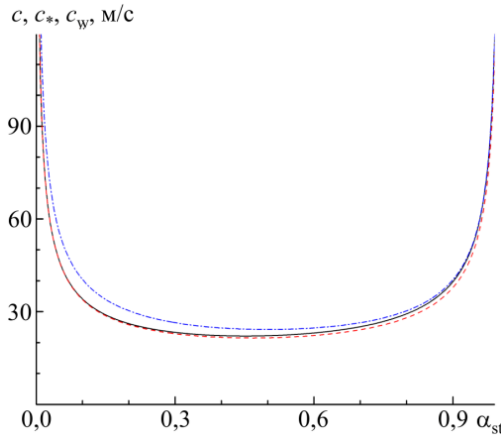


**Fig. 1.** Dependences  $c(\alpha_{st})$  – solid curve,  $c_*(\alpha_{st})$  – dashed curve,  $c_w(\alpha_{st})$  – dash-dotted curve.

Figure 1 shows the dependences of the speeds of sound  $c$  on  $\alpha_{st}$  for a steam-water mixture ( $\rho_s^0 = 1000$  kg/m<sup>3</sup>) under normal conditions, as well as the curve  $c_w(\alpha_{st})$  calculated using Wood's formula [20]

$$c_w^2 = c_{st}^2 \frac{\rho_{st}}{\alpha_{st} \rho}, \quad \text{where } c_{st}^2 = \frac{\gamma_{st}(P + P_{st})}{\rho_{st}^0(1 - b_{st}\rho_{st}^0)}.$$

It can be seen from the figure that the sound velocities in a liquid, taking into account phase transformations, calculated using relations (6) and (7), turn out to be close but somewhat lower than that given by Wood's formula.

### 3. Multidimensional nodal method of characteristics

Let us consider a small time interval, namely, the time integration step for system (5). Changes in the parameters that occur over this short period of time can be found by summing up the local changes that occur in individual coordinate directions. In other words, in order to find an approximate solution of system (5) for a specified time interval, the subsystem is first solved

$$\begin{aligned} \frac{\partial \rho}{\partial t} + u \frac{\partial \rho}{\partial x} + \rho \left( \frac{\partial u}{\partial x} + \frac{v}{r} \right) &= 0, & \frac{\partial u}{\partial t} + u \frac{\partial u}{\partial x} + \frac{1}{\rho} \frac{\partial p}{\partial x} &= 0, & \frac{\partial v}{\partial t} + u \frac{\partial v}{\partial x} &= 0, \\ \frac{\partial p}{\partial t} + u \frac{\partial p}{\partial x} + \rho c^2 \left( \frac{\partial u}{\partial x} + \frac{v}{r} \right) &= \Pi, & \frac{\partial \alpha_s}{\partial t} + u \frac{\partial \alpha_s}{\partial x} + \alpha_s \left( \frac{\partial u}{\partial x} + \frac{v}{r} \right) &= -\frac{J}{\rho_s^0}, & & (8) \\ \frac{\partial \theta_s}{\partial t} + u \frac{\partial \theta_s}{\partial x} + \frac{p}{c_{v,s}\rho_s^0} \left( \frac{\partial u}{\partial x} + \frac{v}{r} \right) &= J \frac{u^2 + v^2}{c_{v,s}\rho_s}, & & & & \end{aligned}$$

which is obtained from (5), in which the terms that change the flow parameters in the direction of the symmetry axis  $Ox$  are retained. Then, after integration (8), based on the new distribution of defining variables, the following subsystem is solved:

$$\begin{aligned} \frac{\partial \rho}{\partial t} + v \frac{\partial \rho}{\partial r} + \rho \left( \frac{\partial v}{\partial r} + \frac{v}{r} \right) &= 0, & \frac{\partial u}{\partial t} + v \frac{\partial u}{\partial r} &= 0, \\ \frac{\partial v}{\partial t} + v \frac{\partial v}{\partial r} + \frac{1}{\rho} \frac{\partial p}{\partial r} &= 0, & \frac{\partial p}{\partial t} + v \frac{\partial p}{\partial r} + \rho c^2 \left( \frac{\partial v}{\partial r} + \frac{v}{r} \right) &= \Pi, & & (9) \\ \frac{\partial \alpha_s}{\partial t} + v \frac{\partial \alpha_s}{\partial r} + \alpha_s \left( \frac{\partial v}{\partial r} + \frac{v}{r} \right) &= -\frac{J}{\rho_s^0}, & \frac{\partial \theta_s}{\partial t} + v \frac{\partial \theta_s}{\partial r} + \frac{p}{c_{v,s}\rho_s^0} \left( \frac{\partial v}{\partial r} + \frac{v}{r} \right) &= J \frac{u^2 + v^2}{c_{v,s}\rho_s}, & & \end{aligned}$$

which takes into account changes along the coordinate direction  $Or$ .

The characteristic equation of subsystem (8) has only real roots:  $\xi_1 = u - c$ ;  $\xi_2 = \xi_3 = \xi_4 = \xi_5 = u$ ;  $\xi_6 = u + c$ . The compatibility relations along the characteristic directions  $dx/dt = u \pm c$  have the form

$$dp \pm \rho c du = \frac{1}{u \pm c} \left( \Pi - \rho c^2 \frac{v}{r} \right) dt. \quad (10)$$

On the trajectory characteristic  $dx/dt = u$ , the equalities

$$dv=0, \quad dp - c^2 d\rho = \Pi, \quad d\alpha_s - \frac{\alpha_s}{\rho} d\rho = -\frac{1}{\rho_s^0} J, \quad c_{v,s} \rho_s^0 d\theta_s - \frac{p}{\rho} d\rho = J \frac{u^2 + v^2}{\alpha_s}, \quad (11)$$

which directly follows from subsystem (8).

Similar relations are also valid for (9). The characteristic equation of subsystem (9) has roots:  $\xi_1 = v - c$ ;  $\xi_2 = \xi_3 = \xi_4 = \xi_5 = v$ ;  $\xi_6 = v + c$ . The compatibility relations along the characteristic directions  $dr/dt = v \pm c$  have the form

$$dp \pm \rho c dv = \frac{1}{v \pm c} \left( \Pi - \rho c^2 \frac{v}{r} \right) dt. \quad (12)$$

On the trajectory characteristic  $dr/dt = v$ , the equalities

$$du=0, \quad dp - c^2 d\rho = \Pi, \quad d\alpha_s - \frac{\alpha_s}{\rho} d\rho = -\frac{1}{\rho_s^0} J, \quad d\theta_s - \frac{p}{\rho c_{v,s} \rho_s^0} d\rho = J \frac{u^2 + v^2}{\alpha_s c_{v,s} \rho_s^0}. \quad (13)$$

Based on the foregoing, when passing from the time step  $t^n$  to  $t^{n+1} = t^n + \Delta t$ , the calculation process is divided into a number of intermediate calculations, on each of which the nodes of the computational domain are first moved along the  $Ox$  axis and in them according to the iterative procedure of the one-dimensional nodal MC [11]:

$$\begin{aligned} \tilde{p}^{(\sigma+1)}(x_k, t^{n+1}) - p_L^{(\sigma)} + (\rho c)_L^{(\sigma)} [\tilde{u}^{(\sigma+1)}(x_k, t^{n+1}) - u_L^{(\sigma)}] &= \left( \frac{\Pi - \rho c^2 v/r}{u + c} \right)_L^{(\sigma)} \Delta t, \\ \tilde{p}^{(\sigma+1)}(x_k, t^{n+1}) - p_R^{(\sigma)} - (\rho c)_R^{(\sigma)} [\tilde{u}^{(\sigma+1)}(x_k, t^{n+1}) - u_R^{(\sigma)}] &= \left( \frac{\Pi - \rho c^2 v/r}{u - c} \right)_R^{(\sigma)} \Delta t, \\ \tilde{p}^{(\sigma+1)}(x_k, t^{n+1}) - p_C^{(\sigma)} - (c_C^{(\sigma)})^2 [\tilde{\rho}^{(\sigma+1)}(x_k, t^{n+1}) - \rho_C^{(\sigma)}] &= \Pi_C^{(\sigma)}, \\ \tilde{\alpha}_s^{(\sigma+1)}(x_k, t^{n+1}) - \alpha_{sC}^{(\sigma)} - \left( \frac{\alpha_s}{\rho_C^{(\sigma)}} \right)_C^{(\sigma)} [\tilde{\rho}^{(\sigma+1)}(x_k, t^{n+1}) - \rho_C^{(\sigma)}] &= -\frac{1}{\rho_s^0} J_C^{(\sigma)}, \\ \tilde{\theta}_s^{(\sigma+1)}(x_k, t^{n+1}) - (\theta_s)_C^{(\sigma)} + \left( \frac{p}{c_{v,s} \rho_s^0 \rho} \right)_C^{(\sigma)} [\tilde{\rho}^{(\sigma+1)}(x_k, t^{n+1}) - \rho_C^{(\sigma)}] &= \frac{1}{c_{v,s} \rho_s^0} \left( J \frac{u^2 + v^2}{\alpha_s} \right)_C^{(\sigma)}, \\ \tilde{v}^{(\sigma+1)}(x_k, t^{n+1}) &= v_C^{(\sigma)}, \end{aligned} \quad (14)$$

where  $\sigma$  is the iteration number; indices L, C and R mark the points of intersection of the characteristics  $dx/dy = u + c$ ,  $dx/dy = c$  and  $dx/dy = u - c$ , released from node  $(x_k, t^{n+1})$  with the time level  $t = t^n$ . As a result, at the  $(n+1)$ -th time step, intermediate values of the mixture parameters  $(\tilde{p}, \tilde{u}, \tilde{v}, \tilde{\rho}, \tilde{\alpha}_s, \tilde{\theta}_s)^{n+1}$  are determined at the internal nodes of the computational domain. Expressions (14) are a finite difference representation of relations (10)–(11). Then, using these found values, by enumerating the nodes along the  $Or$  axis, the final values  $(p, u, v, \rho, \alpha_s, \theta_s)^{n+1}$  are calculated by applying the one-dimensional nodal MC procedure in the direction of the  $Or$  axis:

$$\begin{aligned} p^{(\sigma+1)}(r_m, t^{n+1}) - \tilde{p}_L^{(\sigma)} + (\tilde{\rho} \tilde{c})_L^{(\sigma)} [v^{(\sigma+1)}(r_m, t^{n+1}) - \tilde{v}_L^{(\sigma)}] &= \left( \frac{\tilde{\Pi} - \tilde{\rho} \tilde{c}^2 \tilde{v}/r}{\tilde{v} + \tilde{c}} \right)_L^{(\sigma)} \Delta t, \\ p^{(\sigma+1)}(r_m, t^{n+1}) - \tilde{p}_R^{(\sigma)} - (\tilde{\rho} \tilde{c})_R^{(\sigma)} [v^{(\sigma+1)}(r_m, t^{n+1}) - \tilde{v}_R^{(\sigma)}] &= \left( \frac{\tilde{\Pi} - \tilde{\rho} \tilde{c}^2 \tilde{v}/r}{\tilde{v} - \tilde{c}} \right)_R^{(\sigma)} \Delta t, \end{aligned}$$

$$\begin{aligned}
p^{(\sigma+1)}(r_m, t^{n+1}) - \tilde{p}_C^{(\sigma)} - (\tilde{c}_C^{(\sigma)})^2 [\rho^{(\sigma+1)}(r_m, t^{n+1}) - \tilde{\rho}_C^{(\sigma)}] &= \tilde{\Pi}_C^{(\sigma)}, \\
\alpha_s^{(\sigma+1)}(r_m, t^{n+1}) - (\tilde{\alpha}_s)_C^{(\sigma)} - \left(\frac{\tilde{\alpha}_s}{\tilde{\rho}}\right)_C^{(\sigma)} [\rho^{(\sigma+1)}(r_m, t^{n+1}) - \tilde{\rho}_C^{(\sigma)}] &= -\frac{1}{\rho_s^0} \tilde{J}_C^{(\sigma)}, \\
\theta_s(r_m, t^{n+1})^{(\sigma+1)} - (\tilde{\theta}_s)_C^{(\sigma)} + \left(\frac{\tilde{p}}{c_{v,s} \rho_s^0 \tilde{\rho}}\right)_C^{(\sigma)} [\rho(r_m, t^{n+1})^{(\sigma+1)} - \tilde{\rho}_C^{(\sigma)}] &= \frac{1}{c_{v,s} \rho_s^0} \left( \tilde{J} \frac{\tilde{u}^2 + \tilde{v}^2}{\tilde{\alpha}_s} \right)_C^{(\sigma)}, \\
u^{(\sigma+1)}(r_m, t^{n+1}) &= \tilde{u}_C^{(\sigma)}.
\end{aligned} \tag{15}$$

Relations (15) are a finite difference representation of equalities (12)–(13).

The mixture parameters at the boundary nodes located on the left end of the disk (on the windward side), which ensure the fulfillment of the impermeability condition, are determined from the expressions:

$$\begin{aligned}
\tilde{p}^{(\sigma+1)}(x_k, t^{n+1}) - p_R^{(\sigma)} + (\rho cu)_R^{(\sigma)} &= \left( \frac{\Pi - \rho c^2 u/r}{u - c} \right)_R^{(\sigma)} \Delta t, \\
\tilde{p}^{(\sigma+1)}(x_k, t^{n+1}) - p_C^{(\sigma)} - (c_C^{(\sigma)})^2 [\tilde{\rho}^{(\sigma+1)}(x_k, t^{n+1}) - \rho_C^{(\sigma)}] &= \Pi_C^{(\sigma)}, \\
\tilde{\alpha}_s^{(\sigma+1)}(x_k, t^{n+1}) - (\alpha_s)_C^{(\sigma)} - \left(\frac{\alpha_s}{\rho_C^{(\sigma)}}\right)_C^{(\sigma)} [\tilde{\rho}^{(\sigma+1)}(x_k, t^{n+1}) - \rho_C^{(\sigma)}] &= -\frac{1}{\rho_s^0} J_C^{(\sigma)}, \\
\tilde{\theta}_s(x_k, t^{n+1})^{(\sigma+1)} - (\theta_s)_C^{(\sigma)} + \left(\frac{p}{c_{v,s} \rho_s^0 \rho}\right)_C^{(\sigma)} [\tilde{\rho}(x_k, t^{n+1})^{(\sigma+1)} - \rho_C^{(\sigma)}] &= \frac{1}{c_{v,s} \rho_s^0} \left( J \frac{u^2 + v^2}{\alpha_s} \right)_C^{(\sigma)}, \\
\tilde{v}^{(\sigma+1)}(x_k, t^{n+1}) &= v_C^{(\sigma)}.
\end{aligned}$$

For boundary nodes on the back side of the disk, similar relations are valid, except for the first one, which should be replaced by the following:

$$\tilde{p}^{(\sigma+1)}(x_k, t^{n+1}) - p_L^{(\sigma)} - (\rho cu)_L^{(\sigma)} = \left( \frac{\Pi - \rho c^2 u/r}{u + c} \right)_L^{(\sigma)} \Delta t.$$

At the nodes on the edge of the disk, the mixture parameters are found from the expressions:

$$\begin{aligned}
p^{(\sigma+1)}(r_m, t^{n+1}) - \tilde{p}_R^{(\sigma)} + (\tilde{\rho} \tilde{c} \tilde{v})_R^{(\sigma)} &= \left( \frac{\tilde{\Pi} - \tilde{\rho} \tilde{c}^2 \tilde{v}/r}{\tilde{v} - \tilde{c}} \right)_R^{(\sigma)} \Delta t, \\
p^{(\sigma+1)}(r_m, t^{n+1}) - \tilde{p}_C^{(\sigma)} - (\tilde{c}_C^{(\sigma)})^2 [\rho^{(\sigma+1)}(r_m, t^{n+1}) - \tilde{\rho}_C^{(\sigma)}] &= \tilde{\Pi}_C^{(\sigma)}, \\
\alpha_s^{(\sigma+1)}(r_m, t^{n+1}) - (\tilde{\alpha}_s)_C^{(\sigma)} - \left(\frac{\tilde{\alpha}_s}{\tilde{\rho}}\right)_C^{(\sigma)} [\rho^{(\sigma+1)}(r_m, t^{n+1}) - \tilde{\rho}_C^{(\sigma)}] &= -\frac{1}{\rho_s^0} \tilde{J}_C^{(\sigma)}, \\
\theta_s(r_m, t^{n+1})^{(\sigma+1)} - (\tilde{\theta}_s)_C^{(\sigma)} + \left(\frac{\tilde{p}}{c_{v,s} \rho_s^0 \tilde{\rho}}\right)_C^{(\sigma)} [\rho(r_m, t^{n+1})^{(\sigma+1)} - \tilde{\rho}_C^{(\sigma)}] &= \frac{1}{c_{v,s} \rho_s^0} \left( \tilde{J} \frac{\tilde{u}^2 + \tilde{v}^2}{\tilde{\alpha}_s} \right)_C^{(\sigma)}, \\
u^{(\sigma+1)}(r_m, t^{n+1}) &= \tilde{u}_C^{(\sigma)}.
\end{aligned}$$

### 3. Numerical simulation results

To test the proposed integration method, we compare the results of numerical calculations obtained using multidimensional nodal MC with the data of a number of self-similar problems. As the first such problem, we consider a flow with a centered rarefaction wave in a flow around a flat plate at an angle  $\delta > 0$  by a uniform gas-liquid mixture flow with  $J = 0$ ,  $\varepsilon_s = \text{const}$  (Fig. 2, *a*). In the indicated figure, *BC* is an impermeable wall,

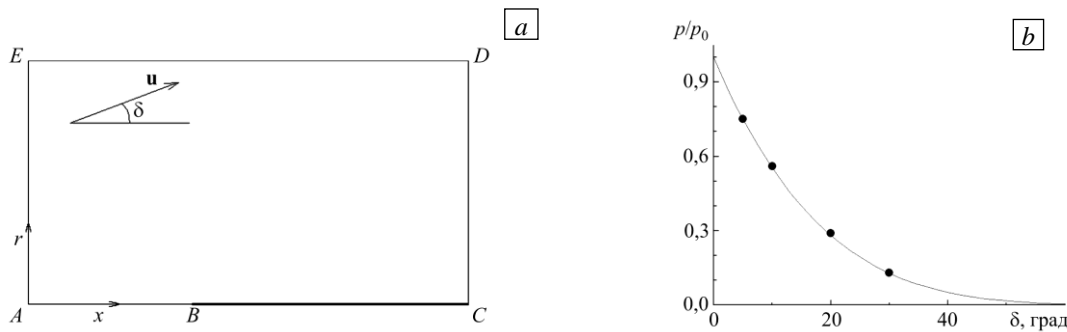
on the remaining boundaries of the computational domain –  $AB$ ,  $CD$ ,  $DE$  and  $EA$ , soft boundary conditions were set – through which the mixture can freely flow in or out. For the problem under consideration, the flow parameters can be found from the system of ordinary differential equations

To test the integration method proposed in the discussed model of a vapor-droplet mixture, we compare the results of numerical calculations obtained using multidimensional nodal MC with the data of solutions of a number of self-similar problems.

**Problem 1.** Let us consider a flow with a centered rarefaction wave with a uniform gas-liquid mixture flow around a flat plate at an angle  $\delta > 0$  with  $J = 0$ ,  $\varepsilon_s = \text{const}$  (Fig. 2a). In the figure,  $BC$  is an impermeable plate; at the remaining boundaries ( $AB$ ,  $CD$ ,  $DE$  and  $EA$ ), the boundary conditions are soft, that is, such that the mixture can freely flow in or out through these boundaries. For the problem under consideration, the flow parameters can be found from the system of ordinary differential equations

$$\begin{aligned} \frac{d\rho}{d\xi} &= -\frac{\rho[u(v-u\xi) + c^2\xi]}{(v-u\xi)^2 + \frac{c^2(1+\xi^2)}{2}\left(\frac{\alpha_s}{1-\alpha_s} + \frac{\rho c^2}{p} - 1\right)} \equiv \Omega, \\ \frac{dp}{d\xi} &= c^2\Omega, \quad \frac{du}{d\xi} = \frac{(v-u\xi)\xi}{\rho(1+\xi^2)}\Omega, \\ \frac{dv}{d\xi} &= -\frac{(v-u\xi)}{\rho(1+\xi^2)}\Omega, \quad \frac{d\alpha_s}{d\xi} = \frac{\alpha_s}{\rho}\Omega, \end{aligned} \quad (16)$$

which is obtained from the flat version of system (5) after introducing the variable  $\xi = r/x$  [21]. This system is integrated from  $\xi = \xi_0 = (M_0^2 - 1)^{-\frac{1}{2}}$  to such a value  $\xi = \xi_1$  at which the flow becomes collinear to the plate surface. Here,  $M_0 = u_0/c_0$  and  $c_0$  are the Mach number and the speed of sound in the unperturbed mixture.



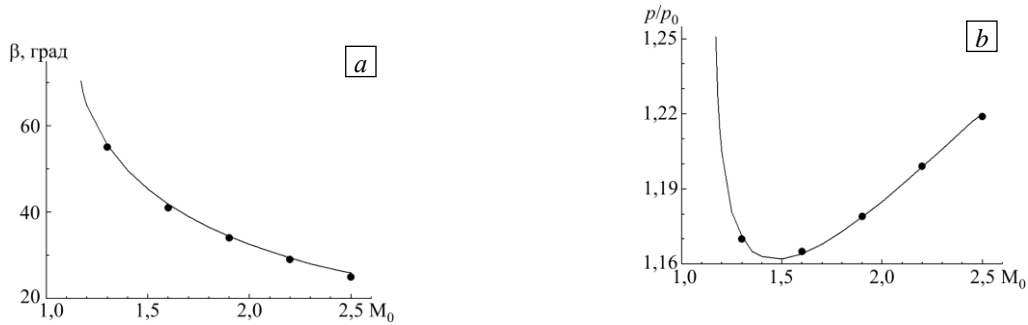
**Fig. 2.** Flow with a centered rarefaction wave: flow diagram (a); dependence of  $p/p_0$  at the barrier on  $\delta$  (b).

Figure 2b shows the dependence  $p=p_0(\delta)$  obtained from system (16). The dots in this figure mark the relative pressures near the solid wall, calculated by the above-described flat version of the multidimensional nodal MC upon reaching the steady flow regime at  $p_0 = 0,1$  MPa,  $\alpha_{s0} = 0,02$  for a water-air mixture ( $\gamma = 1,4$ ;  $\rho_{g0} = 1,16$  kg/m<sup>3</sup>;  $\rho_{s0} = 1000$  kg/m<sup>3</sup>) on a grid of  $300 \times 300$  nodes. We note the coincidence of the results of numerical calculations with the self-similar solution (solid curve).

If the angle  $\delta < 0$ , then in this case, the regime with an attached shock (with an angle of inclination  $\beta$  to the  $Ox$  axis) is realized, the flow parameters behind which, like the angle  $\beta$  itself, can be found from the system of nonlinear algebraic equations

$$\begin{aligned} \rho_{sh} &= \rho_0 \frac{\text{tg}\beta}{\text{tg}(\beta - \delta)}, \quad \frac{\alpha_{s,sh}}{\alpha_{s0}} = \frac{\rho_{sh}}{\rho_0}, \\ p_{sh} &= p_0 + \rho_0 c_0^2 M_0^2 \sin^2 \beta \left[ 1 - \frac{\text{tg}(\beta - \delta)}{\text{tg}\beta} \right], \\ \frac{\rho_0}{\rho_{sh}} &= 1 - \frac{2(1 - \alpha_{s0})(p_{sh} - p_0)}{p_0(\gamma - 1) + p_{sh}(\gamma + 1)}, \end{aligned} \quad (17)$$

which are the Rankine–Hugoniot relations written in the direction orthogonal to the front of the attached shock, considered together with the expression for the shock adiabat of the mixture [22].



**Fig. 3.** Flow with an attached shock:  $\beta(M_0)$  (a) и  $p/p_0(M_0)$  (b). Solid curves – self-similar solution, dots – data of numerical calculations.

In Fig. 3,  $a - b$  solid curves mark the dependences  $\beta(M_0)$ ,  $p = p_0(M_0)$ , obtained from the system of equations (17) at  $p_0 = 0,1$  MPa,  $\alpha_{s0} = 0,02$ , and  $\delta = -3^0$  for water-air mixtures. On the same plots, the dots mark the results of numerical simulation calculated using the MUCM on a grid of  $500 \times 500$  nodes with a Courant number of 1,19. Note the coincidence of the calculated data with the self-similar solution.

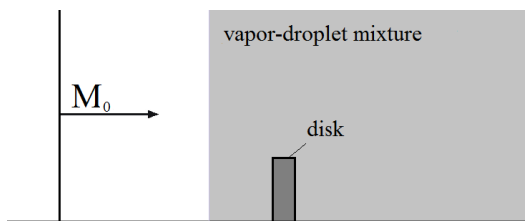


**Fig. 4.** Scheme for the problem of the interaction of a shock wave with a disk in a vapor-drop mixture.

**Problem 2.** Let us consider the shock wave falling on the disk (Fig. 4), moving through the vapor without drops. The disk is located in a half-space filled with a vapor-droplet mixture with  $p_0 = 0,1$  MPa;  $\alpha_{s0} = 0,01$ ;  $n = 10^9 \text{ m}^{-3}$ ; and  $\theta_{s0} = 375$  K. The physical and thermodynamic characteristics of water droplets are as follows:  $\rho_s^0 = 1000 \text{ kg/m}^3$ ;  $\lambda_s = 56,4 \times 10^{-2} \text{ kg m/(s}^3 \text{ K)}$ ;  $c_s = 4,22 \times 10^3 \text{ m}^2/(\text{s}^2 \text{ K)}$ ;  $h = 2,3 \times 10^6 \text{ J/kg}$ ; and  $\Delta\theta_s = 0$ . The properties of water vapor were determined using the thermal and caloric equations of

state (7). The pressure, velocity, and density of the vapor behind the shock wave front in the gas fraction (with index sh) were calculated from the relations

$$\rho_{st,sh}^0 = \rho_{st,0}^0 \frac{R_{st} + 2c_{v,st}}{R_{st} + \frac{2c_{v,st}}{M_0^2}}, \quad u_{sh} = \frac{2c_{v,st}c_0}{R_{st} + 2c_{v,st}} \left( M_0 - \frac{1}{M_0} \right), \quad p_{sh} = \frac{p_0}{R_{st} + 2c_{v,st}} \left[ 2M_0^2 (R_{st} + c_{v,st}) - R_{st} \right],$$

where  $c_0$  and  $M_0 = D/c_0$  are the speed of sound in the undisturbed steam and the Mach number ( $D$  is the velocity of the shock wave front), respectively. A shock wave moving in a dusty space is formed as a result of the interaction of a shock wave moving along a vapor with a contact boundary separating pure and dusty gases.

Figure 5,  $a - b$  shows the distributions of pressure  $p/p_0$ , volume fraction of the dispersed fraction  $\alpha_s$  by the time  $t = 0,087$  s, obtained in the calculation at the Mach number  $M_0 = 1,5$ . The calculations were carried out on a grid of  $400 \times 100$  nodes. Note the absence of droplet evaporation during the entire calculation time, including behind the disk. This is because for this problem, the pressure in the entire computational domain always exceeds the initial value  $p_0$ , and therefore, the saturation temperature always exceeds the liquid temperature, as a result of which there is no boiling of droplets. We also note the presence of damped pressure oscillations at the end of the disk from its windward side near the symmetry axis (Fig. 5,  $e$ ).

**Problem 3.** As a problem in which explosive evaporation of drops is observed, the flow of a vapor-drop mixture near a disk is considered. The disc is instantly placed in a homogeneous flow of a dispersed medium with the following parameters: 0,1 MPa;  $\alpha_{s0} = 0,01$ ;  $n = 10^9 \text{ m}^{-3}$ ;  $\theta_{s0} = 375$  K, and moves along the axis of symmetry with a speed of  $u_0 = 20$  m/s. The calculations were carried out on a grid with  $100 \times 100$  nodes.

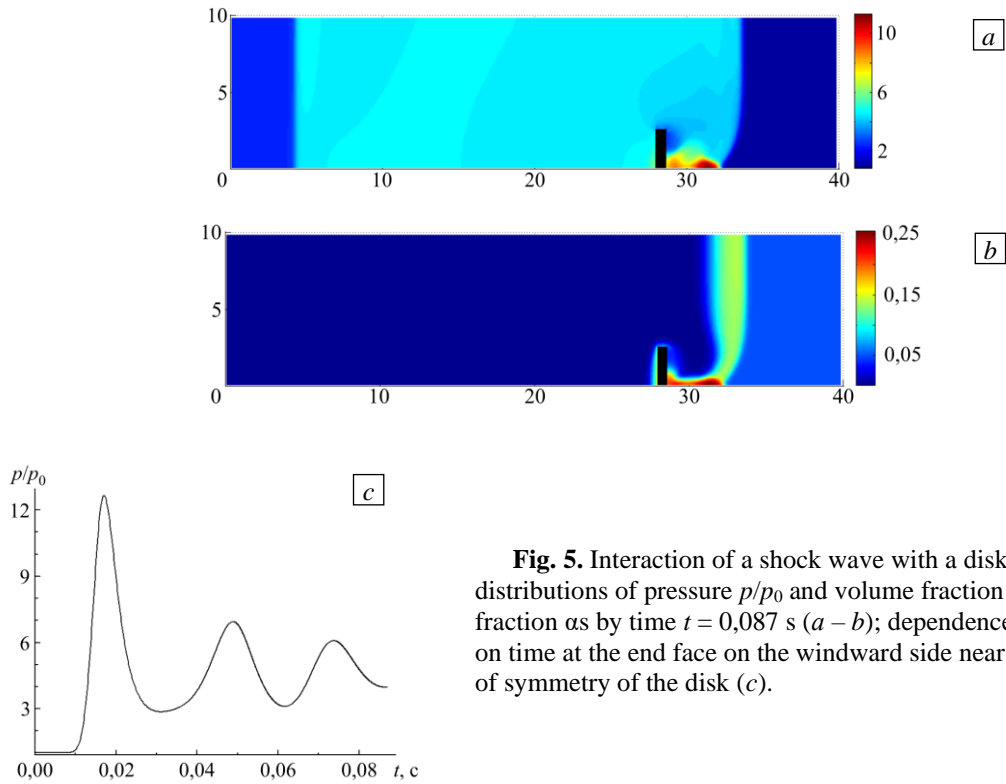


**Fig. 5.** Interaction of a shock wave with a disk: distributions of pressure  $p/p_0$  and volume fraction of liquid fraction  $\alpha_s$  by time  $t = 0,087$  s ( $a - b$ ); dependence of  $p/p_0$  on time at the end face on the windward side near the axis of symmetry of the disk ( $c$ ).

Figure 6 shows the calculated data on the distribution of the relative pressure and volume fraction of the liquid fraction, as well as the saturation temperature near the disk, obtained by the time  $t = 0,045$  s. Since the temperature of the droplets is higher than the saturation temperature, which, as seen from Fig. 6c, has a value of 374 K, intensive droplet evaporation is observed behind the disk.

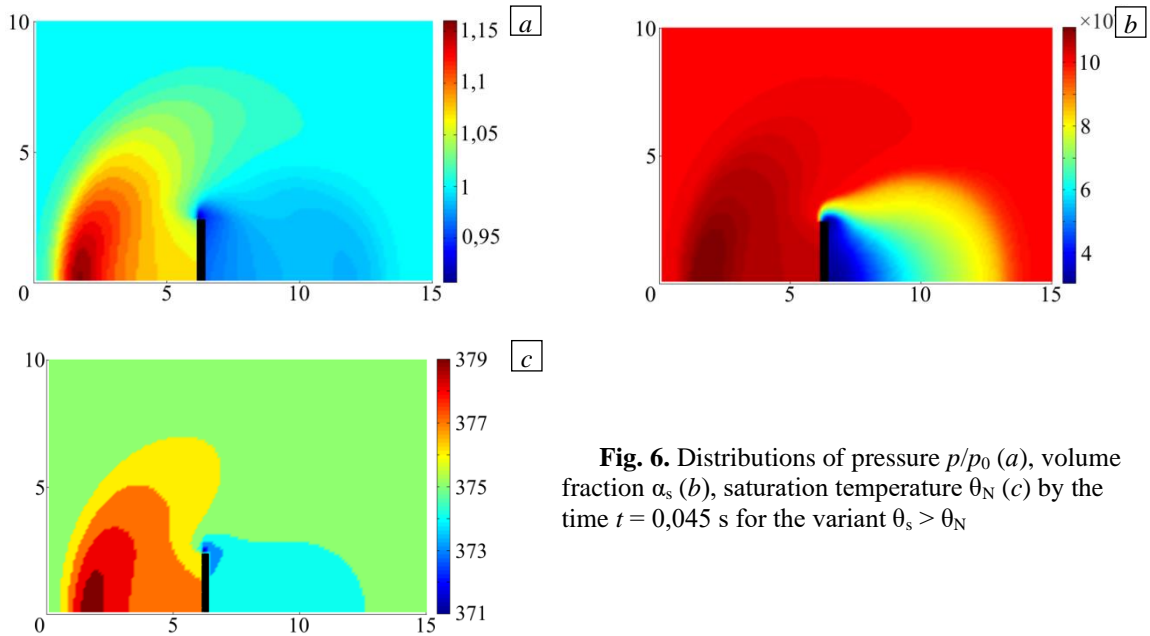


**Fig. 6.** Distributions of pressure  $p/p_0$  ( $a$ ), volume fraction  $\alpha_s$  ( $b$ ), saturation temperature  $\theta_N$  ( $c$ ) by the time  $t = 0,045$  s for the variant  $\theta_s > \theta_N$

Problem 4. Figure 7 shows the results of calculating the flow around the disk for the same initial data as in problem 3, but with the initial temperature of the drops  $\theta_{s0} = 315$  K. In this case, the temperature of the drops behind the disk is below the marked level of 374 K, so there is no evaporation of the drops, and the flow differs significantly from that considered above with the explosive evaporation of droplets behind the disk.

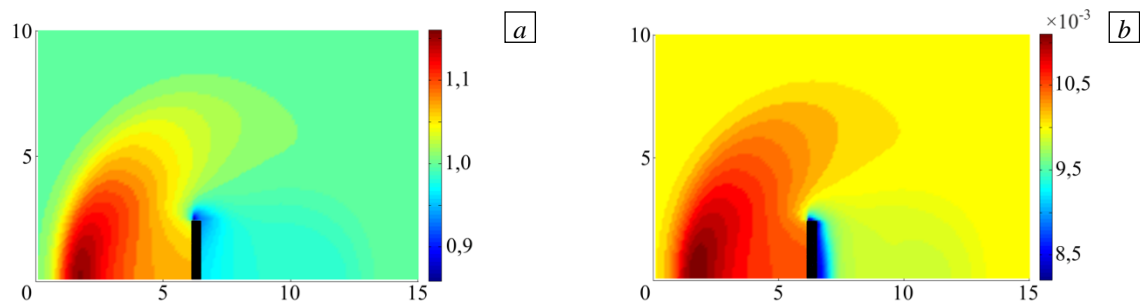


Fig. 7. Distributions of pressure  $p/p_0$  (a), volume fraction  $\alpha_s$  (b) for  $\theta_s < \theta_N$

#### 4. Conclusion

A hyperbolic model of a vapor-droplet mixture is presented, which takes into account the evaporation of drops by an explosive mechanism. It is a development of the generalized-equilibrium mixture model. The liquid fraction is assumed to be incompressible. In the model used, it is assumed that the phase transition in the process of intense droplet evaporation occurs under conditions of an overheated state when the liquid temperature exceeds the saturation temperature. A characteristic analysis of the model equations is carried out, and their hyperbolicity is shown. An analytical formula is obtained for calculating the speed of sound in a vapor-drop mixture. It is noted that the value of the speed of sound in the mixture in the presence of phase transformations turns out to be somewhat lower than that given by Wood's formula.

A multidimensional nodal characteristic method is described for integrating hyperbolic systems, according to which the original system of equations is split into a number of one-dimensional subsystems. For each of the subsystems, differential relations are derived that are valid in the characteristic directions. When solving one-dimensional problems, an iterative algorithm of the inverse method of characteristics is applied. The algorithm has been tested on plane problems with self-similar solutions, such as the flow of a uniform flow near a plate with an attached shock wave and flow with a centered rarefaction wave. This calculation method was used to study the flow of a vapor-droplet near the disk.

It is shown that when a shock interacts with a disk surrounded by a vapor-droplet mixture, no evaporation of drops by the mechanism of explosive boiling is observed. Intensive boiling of drops behind the disk takes place when the disk is instantly placed in a vapor-droplet flow with an initial droplet temperature exceeding the saturation temperature. In this case, the explosive boiling of liquid droplets significantly changes the pattern of the flow around the disk, which must be taken into account when solving problems with such a physical phenomenon.

#### References

1. Surov V.S. On equations of a one-velocity heterogeneous medium. *J. Eng. Phys. Thermophys.*, 2009, vol. 82, pp. 75-84. <https://doi.org/10.1007/s10891-009-0163-3>
2. Surov V.S. Analysis of wave phenomena in gas-liquid media. *High Temp.*, 1998, vol. 36, no. 4, pp. 600-606.
3. Surov V.S. On hyperbolization of a number of continuum mechanics models. *J. Eng. Phys. Thermophys.*, 2019, vol. 92, pp. 1302-1317. <https://doi.org/10.1007/s10891-019-02046-x>
4. Surov V.S. A hyperbolic model of boiling liquid. *J. Appl. Mech. Tech. Phys.*, 2020, vol. 61, pp. 1153-1159. <https://doi.org/10.1134/S0021894420070160>
5. Surov V.S. Calculation of quasi-dimensional flows of boiling liquid. *Vychisl. mekh. splosh. sred – Computational continuum mechanics*, 2019, vol. 12, no. 3, pp. 325-333. <https://doi.org/10.7242/1999-6691/2019.12.3.28>
6. Wang Y., Yang V. Vaporization of liquid droplet with large deformation and high mass transfer rate, I: constant-density, constant-property case. *J. Comput. Phys.*, 2019, vol. 392, pp. 56-70. <https://doi.org/10.1016/j.jcp.2019.03.013>
7. Pinhasi G.A., Ullmann A., Dayan A. 1D plane numerical model for boiling liquid expanding vapor explosion (BLEVE). *Int. J. Heat Mass Trans.*, 2007, vol. 50, pp. 4780-4795. <https://doi.org/10.1016/j.ijheatmasstransfer.2007.03.016>
8. Schlottke J., Weigand B. Direct numerical simulation of evaporating droplets. *J. Comput. Phys.*, 2008, vol. 227, pp. 5215-5237. <https://doi.org/10.1016/j.jcp.2008.01.042>
9. Surov V.S. Numerical simulation of the interaction of an air shock wave with a surface gas–dust layer. *J. Eng. Phys. Thermophys.*, 2018, vol. 91, no. 2, pp. 370-376. <https://doi.org/10.1007/s10891-018-1758-3>
10. Magomedov K.M., Kholodov A.S. *Setochno-kharakteristicheskiye chislennyye metody* [Grid-characteristic numerical methods]. Moscow, Nauka, 1988. 287 c.

11. Surov V.S. Multidimensional nodal method of characteristics for hyperbolic systems. *Komp'yuternyye issledovaniya i modelirovaniye – Computer Research and Modeling*, 2021, vol. 13, no. 1, pp. 19-32. <https://doi.org/10.20537/2076-7633-2021-13-1-19-32>
12. Nakamura T., Tanaka R., Yabe T., Takizawa K. Exactly conservative semi-Lagrangian scheme for multi-dimensional hyperbolic equations with directional splitting technique. *J. Comput. Phys.*, 2001, vol. 174, pp. 171-207. <https://doi.org/10.1006/jcph.2001.6888>
13. Yanenko N.N. *Metod drobnykh shagov resheniya mnogomernykh zadach matematicheskoy fiziki* [Method of fractional steps to solve multidimensional problems of mathematical physics]. Novosibirsk, Nauka, 1967. 196 c.
14. Surov V.S. Boiling liquid model. *Vychislitel'nyye tekhnologii – Computational technologies*, 2020, vol. 25, no. 1, pp. 39-48. <https://doi.org/10.25743/ict.2020.25.1.003>
15. Ivashnev O.E. Boiling spokes in nozzles. *Fluid Dyn.*, 2009, vol. 44, pp. 698-717. <https://doi.org/10.1134/s0015462809050081>
16. Bolotnova R.Kh., Buzina V.A., Galimzyanov M.N., Shagapov V.Sh. Gidrodinamicheskiye osobennosti protsessov istecheniya vskipayushchey zhidkosti [Hydrodynamic features of efflux of boiling liquid]. *T i A – T and A*, 2012, vol. 19, no. 6, pp. 719-730.
17. Kulikovskiy A.G., Pogorelov N.V., Semenov A.Yu. *Matematicheskiye voprosy chislennogo resheniya giperbolicheskikh sistem uravneniy* [Mathematical problems in the numerical solution of hyperbolic systems of equations]. Moscow, Fizmatlit, 2001. 608 p.
18. Saurel R., Boivin P., Lemétayer O. A general formulation for cavitating, boiling and evaporating flows. *Comput. Fluid.*, 2016, vol. 128, pp. 53-64. <https://doi.org/10.1016/j.compfluid.2016.01.004>
19. Nigmatulin R.I., Bolotnova R.Kh. Wide-range equation of state of water and steam: Simplified form. *High Temp.*, 2011, vol. 49, pp. 303-306. <https://doi.org/10.1134%2FS0018151X11020106>
20. Wallis G.B. *One-dimensional two-phase flow*. McGraw-Hill Book Company, 1969. 408 p.
21. Surov V.S. Certain self-similar problems of flow of a one-velocity heterogeneous medium. *J. Eng. Phys. Thermophys.*, 2007, vol. 80, pp. 1237-1246. <https://doi.org/10.1007/s10891-007-0160-3>
22. Surov V.S. Shock adiabat of a one-velocity heterogeneous medium. *J. Eng. Phys. Thermophys.*, 2006, vol. 79, pp. 886-892. <https://doi.org/10.1007/s10891-006-0179-x>

*The authors declare no conflicts of interest.*

*Received 22.01.2022; after revision 18.03.2022; accepted for publication 31. 03.2022*